



Published in final edited form as:

*J Phys Chem Lett.* 2019 July 18; 10(14): 3836–3842. doi:10.1021/acs.jpcllett.9b01267.

## Monolayer Sensitivity Enables a 2D IR Spectroscopic Immuno-biosensor for Studying Protein Structures: Application to Amyloid Polymorphs

Joshua S. Ostrander<sup>†</sup>, Justin P. Lomont<sup>†</sup>, Kacie L. Rich<sup>†</sup>, Vivek Saraswat<sup>‡</sup>, Benjamin R. Feingold<sup>‡</sup>, Megan K. Petti<sup>†</sup>, Erin R. Birdsall<sup>†</sup>, Michael S. Arnold<sup>‡</sup>, Martin T. Zanni<sup>\*†</sup>

<sup>†</sup>Department of Chemistry, University of Wisconsin—Madison, Madison, Wisconsin 53706, United States

<sup>‡</sup>Department of Materials Science and Engineering, University of Wisconsin—Madison, Madison, Wisconsin 53706, United States

### Abstract

Immunosensors use antibodies to detect and quantify biomarkers of disease, though the sensors often lack structural information. We create a surface-sensitive two-dimensional infrared (2D IR) spectroscopic immunosensor for studying protein structures. We tether antibodies to a plasmonic surface, flow over a solution of amyloid proteins, and measure the 2D IR spectra. The 2D IR spectra provide a global assessment of antigen structure, and isotopically labeled proteins give residue-specific structural information. We report the 2D IR spectra of fibrils and monomers using a polyclonal antibody that targets human islet amyloid polypeptide (hIAPP). We observe two fibrillar polymorphs differing in their structure at the G24 residue, which supports the hypothesis that hIAPP polymorphs form from a common oligomeric intermediate. This work provides insight into the structure of hIAPP, establishes a new method for studying protein structures using 2D IR spectroscopy, and creates a spectroscopic immunoassay applicable for studying a wide range of biomarkers.

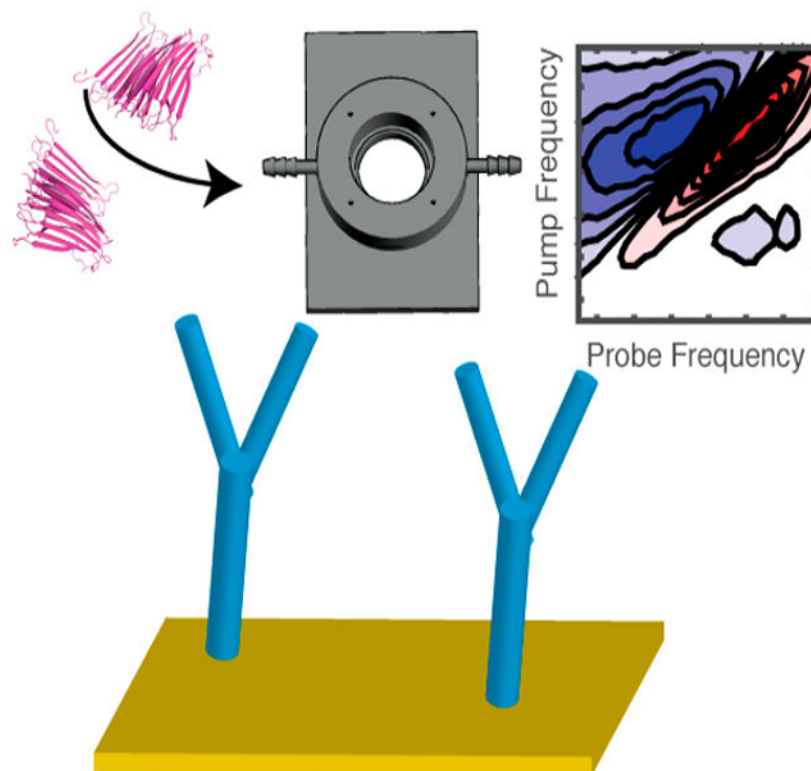
### Graphical Abstract

\*Corresponding Author zanni@chem.wisc.edu.

Supporting Information

The Supporting Information is available free of charge on the ACS Publications website at DOI: [10.1021/acs.jp-cllett.9b01267](https://doi.org/10.1021/acs.jp-cllett.9b01267). Experimental methods, including details of the spectroscopic methods, sample preparation, and control experimental spectra (PDF)

The authors declare the following competing financial interest(s): M.T.Z. is a co-owner of PhaseTech Spectroscopy, Inc., which manufactures pulse shapers and 2D spectrometers like those used in this work.



Immunosensors use antibodies to isolate an antigen, often a protein or other biomarker of interest, from a complex solution. These assays often rely on colorimetric,<sup>1</sup> fluorescence,<sup>2</sup> or electrochemical detection.<sup>3</sup> Consequently, the information obtained is limited to the presence and amount of antigen present. Some antibodies can be crystallized in the presence of an antigen for crystallography,<sup>4</sup> but often no direct structural information is relayed by an immunoassay. Antibodies are typically grown by injecting the protein of interest into an animal, such as a rabbit, and the resulting antibodies are harvested. Polyclonal antibodies bind to a distribution of protein structures,<sup>5</sup> which Ma et al. have invoked as an explanation for why there are not more crystallography studies of amyloid proteins using such an approach.<sup>6</sup> Indeed, particular populations of polymorphs might be linked to the disease, and thus, a structural assay could be invaluable.<sup>7-9</sup>

Almost all two-dimensional infrared (2D IR) spectroscopy experiments have been carried out in bulk solutions. Through a combination of technical advances, it has recently become possible to measure the 2D IR spectrum of a monolayer of molecules using plasmonic enhancement provided by metallic nanostructures. Some plasmonic enhancements have been reported to improve the 2D IR signal strength by  $10^2$ – $10^3$ , alleviating the need for bulk samples.<sup>10-13</sup> Significant enhancements can also be obtained at interfaces using reflection detection.<sup>14</sup> These two methods can also be combined to afford an even larger enhancement.<sup>13</sup> In this report, we extend these recent technological advances to antibody surfaces, inspired by the work of the Gerwert group.<sup>8,9,15</sup> The Gerwert group utilized attenuated total reflection (ATR) Fourier transform infrared (FTIR) spectroscopy to measure the infrared spectrum of an antibody–antigen complex immobilized on a surface.<sup>8,9</sup> They found a

correlation between the maximum frequency of the IR spectrum of the amide I and amide II bands and the progression of Alzheimer's disease, presumably due to a change in the distribution of protein structures. In this Letter, we extend the antibody assay to detection via plasmonically enhanced 2D IR spectroscopy. 2D IR spectroscopy has a number of advantages over ATR or other linear IR spectroscopies.<sup>16-18</sup> Besides frequencies, 2D IR spectroscopy measures cross peaks and diagonal anharmonicities that are sensitive to structure. It also contains 2D lineshapes that reflect the structure and dynamics of the surrounding environment.<sup>19</sup> The signal strength also scales very differently from linear IR spectroscopy. 2D IR spectroscopy scales quadratically, rather than linearly, with extinction coefficient, which enhances the signals of excitonically delocalized vibrational modes that occur in  $\alpha$ -helices,  $\beta$ -sheets, and other secondary structures.<sup>19,20</sup> 2D IR spectroscopy provides a number of observables that are complementary to ATR and other linear IR spectroscopies.

The newfound ability to measure monolayers with 2D IR spectroscopy makes these experiments possible. To measure 2D IR spectra of an antigen bound to an antibody, an accurate background spectrum must be collected to remove unwanted signals from the antibodies and surface-passivating proteins. For this, a flow cell is needed to monitor the same spot on the sample. This enables a precise measurement of the background with and without the presence of antigen under identical conditions, analogous to ATR-FTIR spectroscopy. Additionally, a flow cell facilitates in situ hydrogen–deuterium exchange, making it possible to use either H<sub>2</sub>O or D<sub>2</sub>O as a solvent.

In this Letter, we present an immuno-multidimensional-infrared biosensor to measure the 2D IR spectrum of human islet amyloid polypeptide (hIAPP).<sup>21</sup> hIAPP is a 37 amino acid hormone secreted in conjunction with insulin. It is an appetite suppressant, but when overexpressed during late-stage type 2 diabetes, it aggregates into amyloid plaques in the islets of the pancreas.<sup>22,23</sup> As with the proteins for many amyloid diseases,<sup>5</sup> the oligomeric intermediates of hIAPP, prior to forming amyloid fibrils, are the cytotoxic species.<sup>22,24-26</sup> Little structural information is known about the oligomers of hIAPP, but we have previously identified a transient oligomeric species with a unique ordered structure by using isotope labeling and 2D IR spectroscopy.<sup>27,28</sup> Transient oligomers are difficult to study because they exist at low concentrations, are in equilibrium with monomers, and are kinetically evolving toward fibrils.<sup>29</sup> By creating an immunosensor using antibodies that are selective for hIAPP, we extract a subset of the protein populations and record their 2D IR spectrum. We establish a new approach for studying protein structures with 2D IR spectroscopy and discover, through measurements of proteins with a single amino acid isotopically labeled, that these particular antibodies selectively trap specific amyloid polymorphs.

The details of the spectroscopic methods and sample preparation are provided in the Supporting Information and have been published previously.<sup>30-32</sup> Figure 1 shows a schematic of the workflow used to create the immunosensor to measure hIAPP. We use 3 nm films of thermally evaporated gold on CaF<sub>2</sub> as the substrates for the immunochemistry.<sup>13</sup> We use the anti-amylin polyclonal antibody (Thermo Fisher Scientific, PA1-37075), which is derived from rabbit anti-IgG and raised against the N-terminal sequence of synthetic hIAPP. The antibody is incubated in the presence of CS<sub>2</sub> in deuterated phosphate buffered saline (PBS,

Fisher Scientific, pH 7.4) for 24 h to chemically link the amine side chains of the lysine residues to the gold surface,<sup>33,34</sup> as shown in Figure 1a,b. The CS<sub>2</sub> reacts with the amine groups, and the thiol links the antibodies to the gold before being rinsed three times with PBS. To prevent nonspecific binding of the amylin, the antibody functionalized substrate is soaked in 1% casein in deuterated buffer for 1 h (Figure 1c), before again being rinsed three times. 2D IR spectra are collected in a pump–probe geometry using a mid-IR pulse shaper as described in the Supporting Information. We also found that PBS buffer as the solvent for antibody tethering gave stronger 2D IR signals than ethanol, used previously.<sup>33</sup> 2D IR spectroscopy also confirmed that the casein saturated all available binding sites (see the Supporting Information). We followed prior protocols but did not optimize the antibody assay nor characterize the kinetics of binding. More efficient binding schemes might improve signal strengths and binding efficiency.<sup>35</sup> Measurements were repeated in triplicate.

The above procedure creates an antibody-coated plasmonic surface with minimal amounts of nonspecific binding. Because the antibody and casein blocking agents are much larger proteins than hIAPP, the background signal is expected to be 10–100 larger than the signal from hIAPP from the estimate of the molecular weight provided by the manufacturer. To remove this background, we use a flow cell. First, a background spectrum is collected, then the analyte is added and a second spectrum is collected, as shown in Figure 1d. As has been established in the FTIR community, extremely small changes in OD can be measured using this approach.<sup>8</sup> A flow cell is particularly important for 2D IR measurements, because the 2D IR signals depend on the overlap of the laser pulses in the sample and other variables that alter the signal magnitude. Thus, a flow cell minimizes systematic subtraction errors. The pump–probe signal strengths measured of the antibody and casein background is 1–3 mOD, with the measured change in OD ( $\Delta$ OD) created by the antigen peptide on the order of 10–100  $\mu$ OD.

With the above procedure, we first tested the immunosensor against an aggregated sample of hIAPP, which we have previously reported on numerous occasions.<sup>27,28,36,37</sup> The antibodies are broad spectrum, which can bind both fibrils and oligomers, so we used solutions with fibrils prepared according to our previous studies.<sup>29,38,39</sup> We aggregated 1 mM hIAPP, synthesized according to previously published methods,<sup>32,40</sup> in buffer overnight to create amyloid fibrils. Amyloid fibrils are extremely stable species, and so under these conditions very small amounts of monomers and oligomers would be expected. The aggregated sample was flowed over the antibody substrate and allowed to bind for 1 h before copious rinsing with deuterated PBS buffer. Figure 2 compares the 2D spectra of the sensor before (a) and after (b) addition and rinsing of the amylin. The peak of the antibody and casein is centered at around 1645 cm<sup>-1</sup>. There is a small excited-state absorption background from the 3 nm gold; this additional background signal is smaller than the amylin signal and not noticeable with the antibody background. Upon addition of the hIAPP, the spectrum broadens to lower frequencies. Subtracting a from b reveals the difference 2D IR spectrum in Figure 2d, which is the spectrum of the hIAPP fibrils bound to the antibody with the antibodies, casein, and the excited-state absorption background eliminated. The difference spectrum is dominated by a peak at 1629 cm<sup>-1</sup> with a minor peak at 1650 cm<sup>-1</sup> from residual disordered residues. These experiments establish that the background from the antibody can be reliably subtracted to give the spectrum of the antigen. Previous measurements on similar immuno-

infrared sensors have shown that the spectral differences can be attributed to the structure change of the antigen.<sup>8,9,15</sup>

In Figure 2e, the 2D IR spectrum is shown for the bulk solution sample of hIAPP fibrils measured above, but prior to passing through the flow cell. Figure 2d,e compares the 2D IR spectra of the hIAPP in the bulk and the subtracted 2D spectrum of the bound peptides. We observe that the bulk and surface spectra have very similar line shapes, with a  $4\text{ cm}^{-1}$  difference in the peak frequency; the solution spectrum is dominated by a peak at  $1625\text{ cm}^{-1}$ , while the bound peptide exhibits a peak at  $1629 \pm 1.8\text{ cm}^{-1}$  from three different measurements. It is possible that the frequency difference is a result of the structure being deformed upon binding to the antibody. However, previous experiments using similar immunosensors have suggested that the binding does not significantly alter the secondary structure.<sup>15</sup> Instead, it is more likely that the antibody binds to a subset of hIAPP structures. The amide I frequency of hIAPP depends on the aggregation conditions, which alter the amyloid fibril structure. For example, the amide I frequency ranges by  $1614\text{--}1624\text{ cm}^{-1}$  depending on the protein concentration under which the fibrils are formed, with higher concentrations typically resulting in a lower frequency, reflecting more ordered  $\beta$ -sheet structure.<sup>41</sup> hIAPP also has fibril polymorphs that exhibit different structural motifs at the Valine-17 position.<sup>38,42</sup> Consequently, there is a natural degree of structural heterogeneity in fibrils that correlates to the amide I frequency. The frequency difference between the bulk- and antibody-bound aggregates likely indicates that the antibody preferentially binds to a subset of aggregate structures.<sup>18,41</sup> Measurements of isotope-labeled amino acids support this hypothesis below.

Isotope labels are often used to obtain residue-specific structural information with FTIR and 2D IR spectroscopy.<sup>43-46</sup> With experiments like these in mind, we measured hIAPP synthesized with a  $^{13}\text{C}^{18}\text{O}$  isotope labeled in the backbone carbonyl of the G24 residue. This label effectively decouples the single amino acid residue from the other amide bonds and shifts the local mode frequency about  $65\text{ cm}^{-1}$ . Isotope labels are often used as a probe of structure<sup>28</sup> and local environment.<sup>47</sup> We again ensured that the isotope-labeled peptide was in a fibrillar structure by aggregating the hIAPP overnight, again at  $1\text{ mM}$  concentration. Figure 3 compares the 2D IR spectra of aggregated hIAPP in solution (a) and the difference spectrum when bound to antibody (b). Interestingly, the spectra are not identical. The solution feature shows a distinct peak at  $1585\text{ cm}^{-1}$ , consistent with our previously published results in the fibril state.<sup>28</sup> Upon binding, we observe two peaks, one at about  $1588\text{ cm}^{-1}$  and another at  $1576\text{ cm}^{-1}$ . Thus, we conclude that the antibodies are binding two conformations of hIAPP, one of which is the majority species in solution. The center frequency of the isotope-labeled region reports on the structure through the magnitude of coupling between residues.<sup>17,19,27</sup> A  $9\text{ cm}^{-1}$  shift indicates a significant change in structure. A similar feature was observed at Ala25 and assigned to a polymorph arising from a second aggregation pathway.<sup>38</sup> The  $1576\text{ cm}^{-1}$  peak indicates that the G24 isotope labels are more strongly coupled compared to the final fibril obtained in solution, in which G24 resides in a disordered loop.<sup>17</sup> These observations are inconsistent with the antibody altering the conformation of a single structure, because one would not expect two different isotope-labeled frequencies. Instead, we conclude that these antibodies are binding at least two different structures and enriching a subpopulation of one polymorphic structure. Additional

labels could be used for a more thorough structural investigation. Additional polymorphs might be observed using different antibodies, if the polymorphs are different in other regions outside of the G24 residue.

We next added hIAPP to the antibody sensor prior to aggregation, before fibrils have formed. The peptide was dissolved in PBS buffer at a concentration of 33  $\mu\text{M}$  and immediately introduced to the antibody sensor. Figure 4 shows the spectrum obtained after subtraction. We observe an inhomogeneously broadened peak at 1646  $\text{cm}^{-1}$  with a small shoulder at about 1660  $\text{cm}^{-1}$ . The 1660  $\text{cm}^{-1}$  feature may be from a  $\beta$ -turn or some other ordered structure.<sup>48</sup> Without antibodies, 33  $\mu\text{M}$  is too low of a concentration to obtain a spectrum of hIAPP in the bulk, but the antibody bound spectrum looks nearly identical to our group's measurements on the early aggregation time scales of hIAPP in bulk solution at a 1 mM concentration.<sup>36</sup> Thus, we conclude that disordered state bound to the antibody is similar to that in solution and that the oligomeric structure studied at 1 mM concentrations with standard transmission 2D IR spectroscopy is equivalent to the oligomeric structures that exist at 33  $\mu\text{M}$ . These experiments validate the use of high-concentration studies for studying oligomer structure.<sup>29</sup>

We previously published data proposing an aggregation mechanism in which all fibrillar polymorphs originate from the same oligomer structure.<sup>38</sup> The data presented here support this hypothesis, because we see no polymorphs when the antibodies are incubated with hIAPP during the lag time, prior to fibril formation when only oligomers are present. Polymorphs are observed when the antibodies are exposed to fibrils, implying that polymorphs arise after formation of the oligomers, consistent with our previous publication.<sup>38</sup> Additional studies with other antibodies might be useful to further test that hypothesis.

We also performed several control experiments. To confirm that the amylin polyclonal antibodies are specific to hIAPP as advertised by the manufacturer, we added a concentrated solution of hen egg white lysozyme (HEWL, 1 mg/mL) and observed no change in the background signal (Supporting Information, Figure S1). Additionally, we added a concentrated solution of hIAPP (~2 mM) with only casein added and no antibody. We observed no nonspecific binding of hIAPP to the casein or bare gold substrate in the difference 2D spectrum (Supporting Information, Figure S2). Thus, the spectra above are indeed generated by hIAPP.

In conclusion, we have presented a 2D IR immuno-biosensor to extract and investigate the structure of hIAPP. We show that 2D IR spectrometers have sufficient signal-to-noise to subtract off the antibody background and can trap hIAPP in both its aggregated and oligomeric structures. The signal-to-noise also enables data collection on singly isotope-labeled polypeptides for residue-specific structural information. For G24-labeled hIAPP, we observe two isotope-labeled peaks, indicating that the antibodies are binding two different fibrillar polymorphs. In contrast, antibodies soaked in hIAPP prior to aggregation produced spectra of oligomers that resembled the bulk solution, supporting a mechanism in which the fibrillar polymorphs arise after a common oligomer structure.<sup>38</sup> There exist many antibodies specific for hIAPP that could be used to further investigate the distribution of polymorphs. Antibodies also exist for many other amyloid-forming proteins to which this technique can



be extended and might be correlated with the progression of the disease.<sup>8</sup> The plasmonic enhancement that enables monolayer sensitivity for immobilized structures at the surface allows for a flow cell to be used for proteins and opens up many new avenues of exciting research using 2D IR spectroscopy. In this publication we focused on fibrillar polymorphs, but this approach is applicable to many other topics. Besides broad-spectrum antibodies like those studied here, conformation-specific antibodies exist. There are antibodies that recognize carbohydrates, lipids, nucleic acids, and small molecules like neurotransmitters. We anticipate that this new advance will enable researchers to use 2D IR spectroscopy to study the structures of proteins from serum and other bodily fluids.

## Supplementary Material

Refer to Web version on PubMed Central for supplementary material.

## ACKNOWLEDGMENTS

Support for this research was provided by NIH through R01DK79895 and R21AG061602. V.S. and M.S.A acknowledge funding by the U.S. Department of Energy, Office of Science, Basic Energy Sciences, under Award No. DE-SC0016007 for gold deposition on CaF<sub>2</sub> substrates. J.P.L. is a Howard Hughes Medical Institute Fellow of the Life Sciences Research Foundation. K.L.R. acknowledges additional support through an NSF Graduate Research Fellowship (Award DGE-1256259). E.R.B. is supported by a fellowship through NIH 5 T32 GM008349. To characterize <sup>13</sup>C<sup>18</sup>O-labeled amino acids a Thermo Q Exactive Plus Mass Spectrometer belonging to the Department of Chemistry at University of Wisconsin—Madison was used and funded by NIH Award 1S10 OD020022-1. The purchase of the Bruker ULTRAFLEX III in 2008 was partially funded by NIH NCRR 1S10RR024601-01 Award to the Department of Chemistry and was used to ensure correct peptide mass.

## REFERENCES

- (1). Liu Y; Liu Y; Mernaugh RL; Zeng X Single Chain Fragment Variable Recombinant Antibody Functionalized Gold Nanoparticles for a Highly Sensitive Colorimetric Immunoassay. *Biosens. Bioelectron* 2009, 24, 2853–2857. [PubMed: 19327975]
- (2). Cui X; Liu M; Li B Homogeneous Fluorescence-Based Immunoassay via Inner Filter Effect of Gold Nanoparticles on Fluorescence of CdTe Quantum Dots. *Analyst* 2012, 137, 3293–3299. [PubMed: 22655288]
- (3). Piro B; Reisberg S Recent Advances in Electrochemical Immunosensors. *Sensors* 2017, 17, 794.
- (4). Griffin L; Lawson A Antibody Fragments as Tools in Crystallography. *Clin. Exp. Immunol* 2011, 165, 285–291. [PubMed: 21649648]
- (5). Kayed R; Leapman RD; Guo Z; Yau W-M; Mattson MP; Tycko R Common Structure of Soluble Amyloid Oligomers Implies Common Mechanism of Pathogenesis. *Science* 2003, 300, 486–489. [PubMed: 12702875]
- (6). Ma B; Zhao J; Nussinov R Conformational Selection in Amyloid-Based Immunotherapy: Survey of Crystal Structures of Antibody-Amyloid Complexes. *Biochim. Biophys. Acta, Gen. Subj* 2016, 1860, 2672–2681.
- (7). Tycko R Amyloid Polymorphism: Structural Basis and Neurobiological Relevance. *Neuron* 2015, 86, 632–645. [PubMed: 25950632]
- (8). Nabers A; Perna L; Lange J; Mons U; Schartner J; Guldenhaupt J; Saum K; Janelidze S; Holleczeck B; Rujescu D; et al. Amyloid Blood Biomarker Detects Alzheimer's Disease. *EMBO Mol. Med.* 2018, 10, No. e8763. [PubMed: 29626112]
- (9). Nabers A; Ollesch J; Schartner J; Kötting C; Genius J; Hafermann H; Klafki H; Gerwert K; Wiltfang J Amyloid- $\beta$ -Secondary Structure Distribution in Cerebrospinal Fluid and Blood Measured by an Immuno-Infrared-Sensor: A Biomarker Candidate for Alzheimer's Disease. *Anal. Chem* 2016, 88, 2755–2762. [PubMed: 26828829]

- (10). Selig O; Siffels R; Rezus YLA Ultrasensitive Ultrafast Vibrational Spectroscopy Employing the Near Field of Gold Nanoantennas. *Phys. Rev. Lett* 2015, 114, 233004. [PubMed: 26196799]
- (11). Kraack JP; Kaech A; Hamm P Surface Enhancement in Ultrafast 2D ATR IR Spectroscopy at the Metal-Liquid Interface. *J. Phys. Chem. C* 2016, 120, 3350–3359.
- (12). Gandman A; Mackin R; Cohn B; Rubtsov IV; Chuntonov L Two-Dimensional Fano Lineshapes in Ultrafast Vibrational Spectroscopy of Thin Molecular Layers on Plasmonic Arrays. *J. Phys. Chem. Lett* 2017, 8, 3341–3346. [PubMed: 28677974]
- (13). Petti MK; Ostrander JS; Saraswat V; Birdsall ER; Rich KL; Lomont JP; Arnold MS; Zanni MT Enhancing the Signal Strength of Surface Sensitive 2D IR Spectroscopy. *J. Chem. Phys* 2019, 150, 024707. [PubMed: 30646693]
- (14). Nishida J; Yan C; Fayer MD Enhanced Nonlinear Spectroscopy for Monolayers and Thin Films in Near-Brewster's Angle Reflection Pump-Probe Geometry. *J. Chem. Phys* 2017, 146, 094201.
- (15). Nabers A; Ollesch J; Schartner J; Kötting C; Genius J; Haußmann U; Klafki H; Wiltfang J; Gerwert K An Infrared Sensor Analysing Label-Free the Secondary Structure of the Abeta Peptide in Presence of Complex Fluids. *J. Biophotonics* 2016, 9, 224–234. [PubMed: 25808829]
- (16). Baiz CR; Tokmakoff A Measuring Protein Structural Heterogeneity with Two-Dimensional Infrared Spectroscopy. *Biophys. J* 2014, 106, 459a–459a. [PubMed: 24461021]
- (17). Lomont JP; Ostrander JS; Ho JJ; Petti MK; Zanni MT Not All  $\beta$ -Sheets Are the Same: Amyloid Infrared Spectra, Transition Dipole Strengths, and Couplings Investigated by 2D IR Spectroscopy. *J. Phys. Chem. B* 2017, 121, 8935–8945. [PubMed: 28851219]
- (18). Lomont JP; Rich KL; Maj M; Ho JJ; Ostrander JS; Zanni MT Spectroscopic Signature for Stable  $\beta$ -Amyloid Fibrils versus  $\beta$ -Sheet-Rich Oligomers. *J. Phys. Chem. B* 2018, 122, 144–153. [PubMed: 29220175]
- (19). Ghosh A; Ostrander JS; Zanni MT Watching Proteins Wiggle: Mapping Structures with Two-Dimensional Infrared Spectroscopy. *Chem. Rev* 2017, 117, 10726–10759. [PubMed: 28060489]
- (20). Remorino A; Hochstrasser RM Three-Dimensional Structures by Two-Dimensional Vibrational Spectroscopy. *Acc. Chem. Res* 2012, 45, 1896–1905. [PubMed: 22458539]
- (21). Cooper GJS; Leighton B; Dimitriadis GD; Parry-Billings M; Kowalchuk JM; Howland K; Rothbard JB; Willis AC; Reid KBM Amylin Found in Amyloid Deposits in Human Type 2 Diabetes Mellitus May Be a Hormone That Regulates Glycogen Metabolism in Skeletal Muscle. *Proc. Natl. Acad. Sci. U. S. A* 1988, 85, 7763–7766. [PubMed: 3051005]
- (22). Abedini A; Cao P; Plesner A; Zhang J; He M; Derk J; Patil SA; Rosario R; Lonier J; Song F; et al. RAGE Binds Preamyloid IAPP Intermediates and Mediates Pancreatic  $\beta$  Cell Proteotoxicity. *J. Clin. Invest* 2018, 128, 682–698. [PubMed: 29337308]
- (23). Shim S-H; Gupta R; Ling YL; Strasfeld DB; Raleigh DP; Zanni MT Two-Dimensional IR Spectroscopy and Isotope Labeling Defines the Pathway of Amyloid Formation with Residue-Specific Resolution. *Proc. Natl. Acad. Sci. U. S. A* 2009, 106, 6614–6619. [PubMed: 19346479]
- (24). Wiltzius JJW; Sievers SA; Sawaya MR; Eisenberg D Atomic Structures of IAPP (Amylin) Fusions Suggest a Mechanism for Fibrillation and the Role of Insulin in the Process. *Protein Sci.* 2009, 18, 1521–1530. [PubMed: 19475663]
- (25). Luca S; Yau W-M; Leapman R; Tycko R Peptide Conformation and Supramolecular Organization in Amylin Fibrils: Constraints from Solid-State NMR †. *Biochemistry* 2007, 46, 13505–13522. [PubMed: 17979302]
- (26). Raleigh D; Zhang X; Hastoy B; Clark A The  $\beta$ -Cell Assassin: IAPP Cytotoxicity. *J. Mol. Endocrinol* 2017, 59, R121–R140. [PubMed: 28811318]
- (27). Maj M; Lomont JP; Rich KL; Alperstein AM; Zanni MT Site-Specific Detection of Protein Secondary Structure Using 2D IR Dihedral Indexing: A Proposed Assembly Mechanism of Oligomeric HIAPP. *Chem. Sci* 2018, 9, 463–474. [PubMed: 29619202]
- (28). Buchanan LE; Dunkelberger EB; Tran HQ; Cheng P-N; Chiu C-C; Cao P; Raleigh DP; de Pablo JJ; Nowick JS; Zanni MT Mechanism of IAPP Amyloid Fibril Formation Involves an Intermediate with a Transient  $\beta$ -Sheet. *Proc. Natl. Acad. Sci. U. S. A* 2013, 110, 19285–19290. [PubMed: 24218609]



- (29). Serrano AL; Lomont JP; Tu LH; Raleigh DP; Zanni MT A Free Energy Barrier Caused by the Refolding of an Oligomeric Intermediate Controls the Lag Time of Amyloid Formation by HIAPP. *J. Am. Chem. Soc* 2017, 139, 16748–16758. [PubMed: 29072444]
- (30). Ghosh A; Serrano AL; Oudenhoven TA; Ostrander JS; Eklund EC; Blair AF; Zanni MT Experimental Implementations of 2D IR Spectroscopy through a Horizontal Pulse Shaper Design and a Focal Plane Array Detector. *Opt. Lett* 2016, 41, 524. [PubMed: 26907414]
- (31). Shim S-H; Zanni MT How to Turn Your Pump-Probe Instrument into a Multidimensional Spectrometer: 2D IR and Vis Spectroscopies via Pulse Shaping. *Phys. Chem. Chem. Phys* 2009, 11, 748–761. [PubMed: 19290321]
- (32). Middleton CT; Woys AM; Mukherjee SS; Zanni MT Residue-Specific Structural Kinetics of Proteins through the Union of Isotope Labeling, Mid-IR Pulse Shaping, and Coherent 2D IR Spectroscopy. *Methods* 2010, 52, 12–22. [PubMed: 20472067]
- (33). Almeida I; Cascalheira AC; Viana AS One Step Gold (Bio)Functionalisation Based on CS<sub>2</sub>-Amine Reaction. *Electrochim. Acta* 2010, 55, 8686–8695.
- (34). Niu Y; Matos AI; Abrantes LM; Viana AS; Jin G Antibody Oriented Immobilization on Gold Using the Reaction between Carbon Disulfide and Amine Groups and Its Application in Immunosensing. *Langmuir* 2012, 28, 17718–17725. [PubMed: 23210719]
- (35). Johnsson B; Löfås S; Lindquist G; Edström Å; Hillgren R-MM; Hansson A Comparison of Methods for Immobilization to Carboxymethyl Dextran Sensor Surfaces by Analysis of the Specific Activity of Monoclonal Antibodies. *J. Mol. Recognit* 1995, 8, 125–131. [PubMed: 7541226]
- (36). Strasfeld DB; Ling YL; Shim S-H; Zanni MT Tracking Fiber Formation in Human Islet Amyloid Polypeptide with Automated 2D-IR Spectroscopy. *J. Am. Chem. Soc* 2008, 130, 6698–6699. [PubMed: 18459774]
- (37). Ling YL; Strasfeld DB; Shim S; Raleigh DP; Zanni MT Two-Dimensional Infrared Spectroscopy Provides Evidence of an Intermediate in the Membrane-Catalyzed Assembly of Diabetic Amyloid. *J. Phys. Chem. B* 2009, 113, 2498–2505. [PubMed: 19182939]
- (38). Buchanan LE; Maj M; Dunkelberger EB; Cheng PN; Nowick JS; Zanni MT Structural Polymorphs Suggest Competing Pathways for the Formation of Amyloid Fibrils That Diverge from a Common Intermediate Species. *Biochemistry* 2018, 57, 6470–6478. [PubMed: 30375231]
- (39). Dunkelberger EB; Buchanan LE; Marek P; Cao P; Raleigh DP; Zanni MT Deamidation Accelerates Amyloid Formation and Alters Amylin Fiber Structure. *J. Am. Chem. Soc* 2012, 134, 12658–12667. [PubMed: 22734583]
- (40). Marek P; Woys AM; Sutton K; Zanni MT; Raleigh DP Efficient Microwave-Assisted Synthesis of Human Islet Amyloid Polypeptide Designed to Facilitate the Specific Incorporation of Labeled Amino Acids. *Org. Lett* 2010, 12, 4848–4851. [PubMed: 20931985]
- (41). Dunkelberger EB; Grechko M; Zanni MT Transition Dipoles from 1D and 2D Infrared Spectroscopy Help Reveal the Secondary Structures of Proteins: Application to Amyloids. *J. Phys. Chem. B* 2015, 119, 14065–14075. [PubMed: 26446575]
- (42). Tycko R Physical and Structural Basis for Polymorphism in Amyloid Fibrils. *Protein Sci.* 2014, 23, 1528–1539. [PubMed: 25179159]
- (43). Mukherjee S; Chowdhury P; DeGrado WF; Gai F Site-Specific Hydration Status of an Amphipathic Peptide in AOT Reverse Micelles. *Langmuir* 2007, 23, 11174–11179. [PubMed: 17910485]
- (44). Torres J; Kukol A; Goodman JM; Arkin IT Site-Specific Examination of Secondary Structure and Orientation Determination in Membrane Proteins: The Peptidic C-13 = O-18 Group as a Novel Infrared Probe. *Biopolymers* 2001, 59, 396–401. [PubMed: 11598874]
- (45). Flanagan JC; Baiz CR Buried Water in a Lipid Membrane Measured with Site-Specific IR Spectroscopy of Transmembrane Peptides. *Biophys. J* 2019, 116, 317a.
- (46). Scheerer D; Chi H; McElheny D; Keiderling TA; Hauser K Isotopically Site-Selected Dynamics of a Three-Stranded  $\beta$ -Sheet Peptide Detected with Temperature-Jump Infrared-Spectroscopy. *J. Phys. Chem. B* 2018, 122, 10445–10454. [PubMed: 30372071]

- (47). Kim YS; Liu L; Axelsen PH; Hochstrasser RM Two-Dimensional Infrared Spectra of Isotopically Diluted Amyloid Fibrils from A $\beta$ 40. Proc. Natl. Acad. Sci. U. S. A 2008, 105, 7720–7725. [PubMed: 18499799]
- (48). Baiz CR; Tokmakoff A Introduction to Protein 2D IR Spectroscopy In Ultrafast Infrared Vibrational Spectroscopy; Fayer MD, Ed.; CRC Press: New York, 2013; pp 361–404.

Author Manuscript

Author Manuscript

Author Manuscript

Author Manuscript

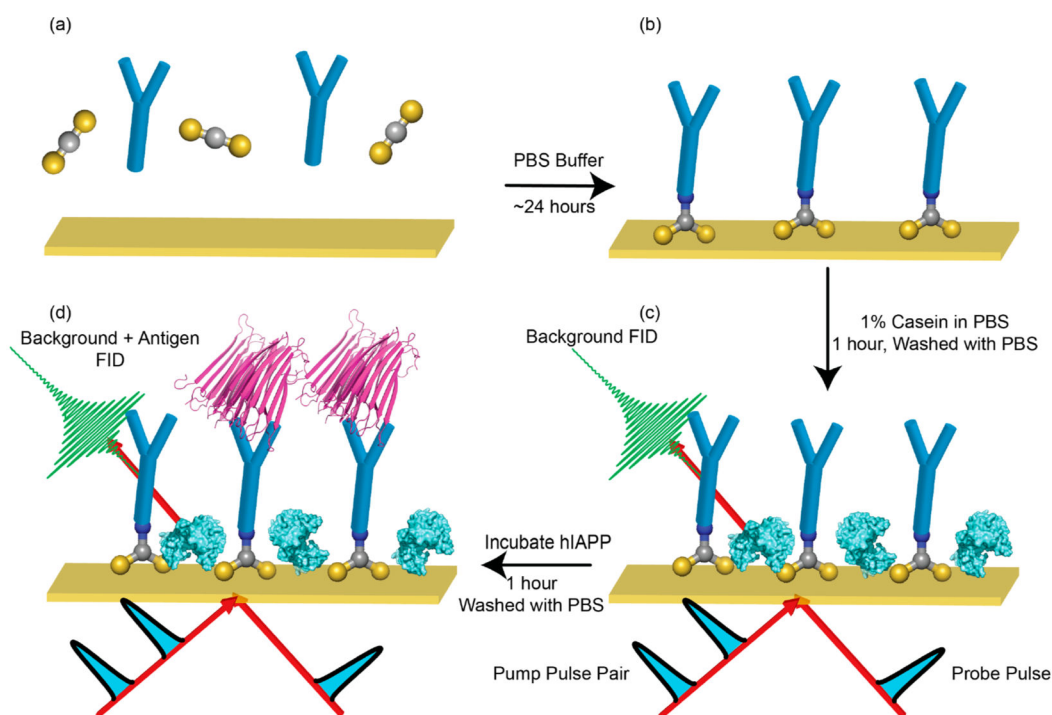


**Figure 1.**

Schematic showing the workflow for the immunochromatography. (a) The gold is soaked with the antibodies and carbon disulfide in PBS buffer for about 24 h. (b) After antibodies are bound to the gold surface, they are rinsed in PBS buffer. (c) A 1% casein solution is then introduced to the flow cell to block any free binding sites. The blocking agents prevent nonspecific adsorption of any proteins, as confirmed in the experiments. At this point, a background transmission 2D IR spectrum is collected. (d) Finally, the hIAPP solution to be analyzed is incubated in the flow cell for 1 h before the sample is washed at least three times with PBS buffer.

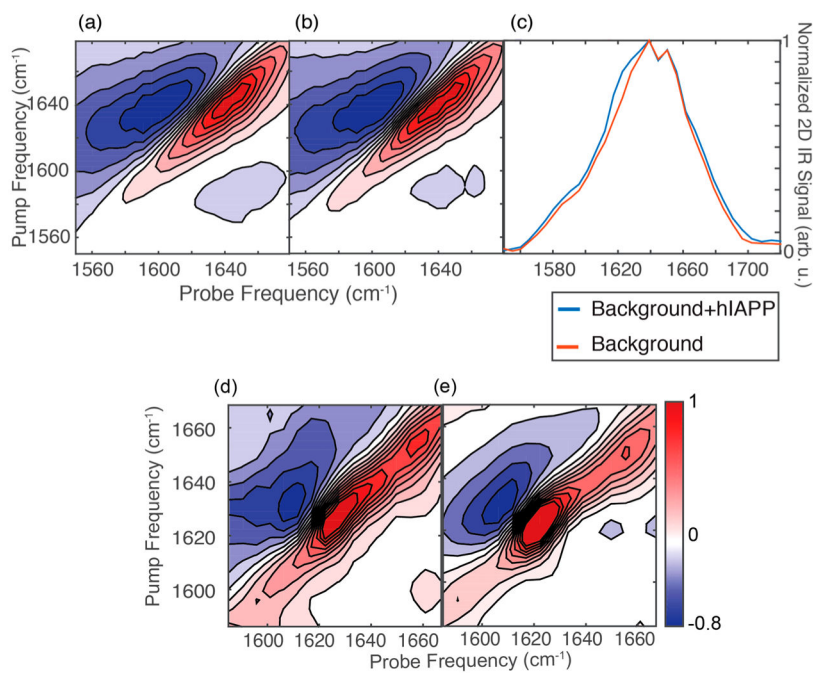


**Figure 2.**

(a) 2D IR spectrum of the antibodies and casein on the gold surface. (b) 2D IR spectrum of the same sensor, but after addition and rinsing of the isotope-labeled amylin solution. (c) Normalized diagonal slices of the 2D spectra shown in panels a and b. (d) 2D IR difference spectrum generated by subtracting panel a from b. (e) Solution 2D IR spectrum of the same amyloid fibrils that bound to the antibody in panel d.

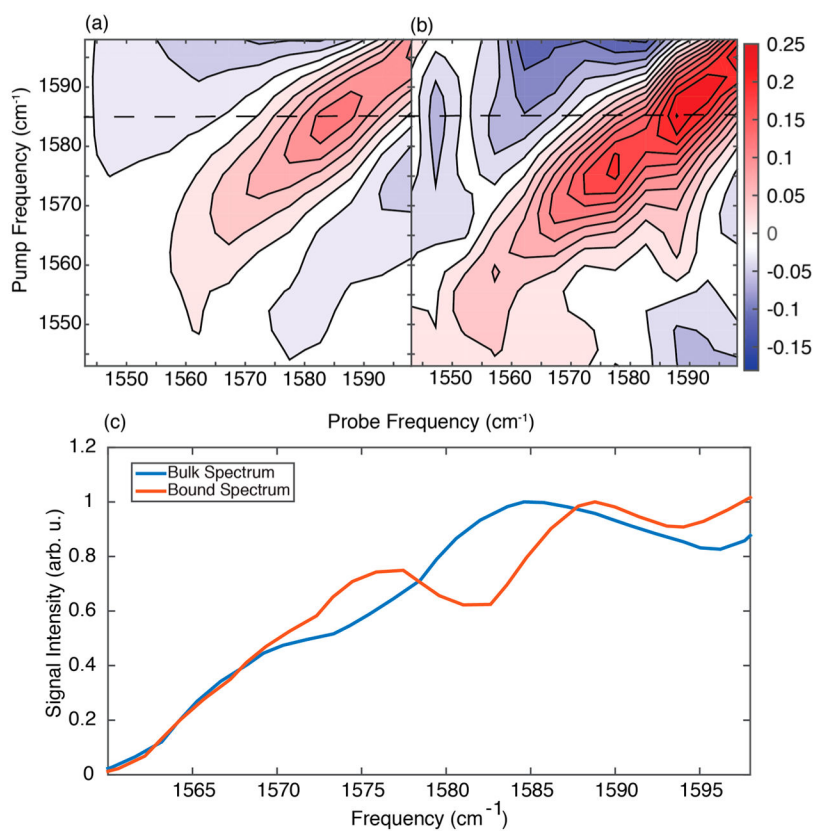


**Figure 3.** (a) Bulk 2D IR spectrum of the G24 label in the aggregated state. (b) Difference spectrum of G24-labeled hIAPP in the isotope-labeled region of the amide-I spectrum. The spectrum is normalized to the most intense diagonal feature. (c) Interpolated diagonal slices of the spectra in panels a and b normalized to the main isotope feature in each spectrum.

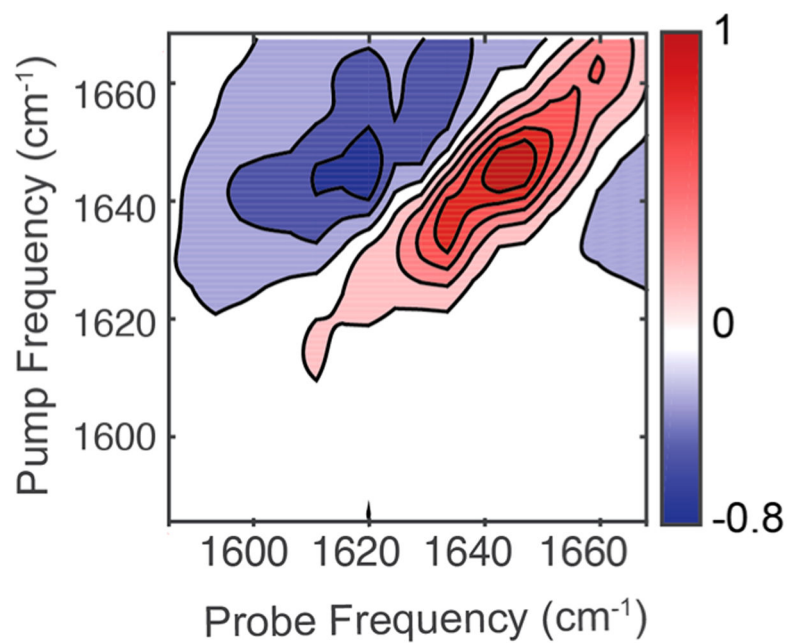


**Figure 4.**  
2D IR difference spectrum of monomeric hIAPP bound to the immunosensor.